

Urban greening based on the supply and demand of atmospheric PM_{2.5} removal



Rui Zhang ^{a,b}, Guojian Chen ^{a,b}, Zhe Yin ^{a,b}, Yuxin Zhang ^b, Keming Ma ^{a,b,*}

^a State Key Laboratory of Urban and Regional Ecology, Research Center for Eco-Environmental Sciences, Chinese Academy of Sciences, Beijing 100085, China

^b University of Chinese Academy of Sciences, Beijing 100049, China

ARTICLE INFO

Keywords:

Urban forestry
Scenario analysis
Ecosystem service
Evergreen greening

ABSTRACT

Faced with various urban environmental problems, cities are implementing greening plans to satisfy the demands of residents for a more habitable environment. Because the relationship between the supply and demand of ecosystem services (ESs) often changes spatially and seasonally, identifying the priority space and suitable species for greening are critical. Taking the removal of particulate matter less than 2.5 μm (PM_{2.5}) in Beijing, China, as an example, a Greening Demand Index was proposed by combining seasonal nongreen coverage, PM_{2.5} concentration, and population density. The results show that, the greening demand (GD) increases along the suburban-urban gradient and is higher in the impervious areas than in other land-cover types. Without considering the seasonal variation in ES supply and demand, the GD will be underestimated in areas with deciduous vegetation coverage. On the one hand, demand comes from scarcity, and on the other hand, demand also comes from inequity. To alleviate the urban-suburban greening demand difference (GDD), greening in impervious areas is the key. To alleviate the seasonal GDD, evergreen greening in the forest and impervious areas is crucial. Forest evergreen greening, which has often been overlooked in the past, should also be considered. Three tree planting scenarios with different species compositions were simulated to evaluate the effects on PM_{2.5} and green distribution. The results indicate that evergreen trees are more efficient in removing atmospheric PM_{2.5} and are indispensable in alleviating the seasonal variation in PM_{2.5} concentration and the spatiotemporally uneven distribution of green. Therefore, they are recommended for greening. This research will provide help for establishing tree planting schemes in urban areas.

1. Introduction

Globally, cities are facing diverse environmental problems, such as air pollution, the heat island effect, and urban water logging, which severely affect the health and life experience of urban residents (Navarrete-Hernandez and Laffan, 2019). Green space (GS) is a crucial urban infrastructure that improves environmental quality by providing various ecosystem services (ESs) (Bolund and Hunhammar, 1999). To alleviate urban environmental problems, many cities worldwide are conducting ambitious tree planting projects, such as Beijing (Yao et al., 2019), London (Tiwary et al., 2009), Baltimore (Bodnaruk et al., 2017), and New York City (Morani et al., 2011). Increasing green in urban areas is a trend for the future.

To achieve higher ES benefits with limited space, identifying the

priority areas for greening is critical. Currently, the GS ESs and human activity demands are unbalanced, and most urban GSs are not used efficiently (Zhong et al., 2020). Some of the previous greening plans used high-resolution images and/or field survey data to find available spaces (Bealey et al., 2007; McDonald et al., 2007; Varol et al., 2019; Wu et al., 2008). To a certain extent, these methods are effective because most of the ESs provided can be available on a large scale (Bolund and Hunhammar, 1999; Lin et al., 2020). However, to maximize the benefits, it is still more meaningful to accurately locate the priority greening areas. Taking tradeoffs between ESs, Bodnaruk et al. (2017) demonstrated a quantitative method for exploring priority tree planting areas. Morani et al. (2011) developed a planting priority index by combining pollution, population, and low canopy cover. Vallecillo et al. (2018) set different spatial constraints to select priority green infrastructure areas

* Corresponding author at: State Key Laboratory of Urban and Regional Ecology, Research Center for Eco-Environmental Sciences, Chinese Academy of Sciences, Beijing 100085, China.

E-mail addresses: zhangrui14@mails.ucas.ac.cn (R. Zhang), pavonina@163.com (G. Chen), zheyin_st@rcees.ac.cn (Z. Yin), yxzheng@rcees.ac.cn (Y. Zhang), mkm@rcees.ac.cn (K. Ma).

with specific goals or strategic plans. Although these studies made urban greening more scientific, the change in ES supply and demand in time or space was still mostly ignored. The supply of ESs is attached to GS, whereas the demand originates from residents and is related to the severity of environmental problems. The uneven distribution of these factors in time and space will lead to changes in the relationship between the supply and demand of ESs. ES supply and demand are often negatively correlated (Wang et al., 2019b; Xu et al., 2020). Places with higher demand and lower supply of ESs should be the priority areas for greening.

Human demand for ESs comes from the lack of services, on the one hand, and inequity in accessing the services on the other. This means that we should focus not only on the greening demand (GD) itself but also on the greening demand difference (GDD). In the space dimension, the imbalance between supply and demand has caused environmental inequity (Wang et al., 2019b; Zhai et al., 2020), which is closely related to the spatial distribution of GS and has been studied in many cities (Nesbitt et al., 2019; Pham et al., 2012; Wang et al., 2019a; Wolch et al., 2014). However, the equity of GS cannot adequately represent the supply and demand relationship of ESs. A fixed GS does not imply an unchanging relationship between the supply and demand of ESs. Because most of the ESs provided by vegetation are through leaves (Givoni, 1991), after defoliation, the ESs provided by plants will decrease rapidly. In the time dimension, the demand for ESs also changes with season. For example, the cooling effect of vegetation is in great need in summer but may not be needed in winter. As the concentrations of most air pollutants are higher in winter than in other seasons (Chen et al., 2015; Wang et al., 2014; Zhao et al., 2019), the demand for air pollutant removal by vegetation often increases in winter. The mismatch between the supply and demand of some ESs often intensifies in the leaf-off season (Yao et al., 2020), which should be considered seriously in greening plans.

Beijing is implementing a tree-protecting project, with alleviating air pollution problems as one of the main objectives (BGGB, 2012). Among all the air pollutants, particulate matter less than 2.5 μm ($\text{PM}_{2.5}$) is the primary pollutant for most of the time in Beijing. Its concentration is much higher than the recommended WHO guidelines (Chen et al., 2015) which seriously affects the health of residents (Song et al., 2017; Zhu et al., 2019). $\text{PM}_{2.5}$ pollution in Beijing is higher in the south and lower in the north (Tian et al., 2018). In contrast, the vegetation coverage is lower in the south and higher in the north (Jiang et al., 2017). As the origin of demand, the population in Beijing is concentrated in the central urban areas (Xu, 2017). The ES supply and demand are clearly mismatched in space. In addition, the $\text{PM}_{2.5}$ concentration is always higher in the leaf-off season than in the leaf-on season (Chen et al., 2015; Zhao et al., 2019). The ES supply and demand also do not match in time. In short, these characteristics make Beijing a typical city with $\text{PM}_{2.5}$ removal an appropriate ES for this study.

The primary aim of this study was to find priority spaces for greening. In addition, to estimate the contribution to environmental inequity, the effect of vegetation coverage in different land-cover types on the GDD in the urban-suburban gradient and between seasons were analyzed. To estimate the effects of tree planting on ES provision and environmental inequity, three tree planting scenarios with different species compositions were simulated.

2. Material and methods

2.1. Quantification and mapping of the GD

In this study, $\text{PM}_{2.5}$ pollution is the target environmental problem to be solved, greening is the method we select to address the problem, people are the ultimate beneficiaries of the greening plan, and $\text{PM}_{2.5}$ removal by GS varies greatly after defoliation. Therefore, to quantify GD, we propose a greening demand index (GDI) by combining geographic information system (GIS) data of nongreen coverage, $\text{PM}_{2.5}$

pollution, and population density in the leaf-on and leaf-off seasons (modified from Morani et al., 2011).

To combine these three factors, each was standardized on a scale of 0 to 1 (Morani et al., 2011). Equal weight was given to the three factors to facilitate the comparison of their contributions to the GDD. The GDI ranges between 0 and 1, and the larger the value is, the higher the demand. The seasonal GDI was calculated as follows:

$$I = ((1 - f) + SPC + SPD)/3 \quad (1)$$

where I is the GDI score of the leaf-off or leaf-on season, f is the green coverage of the corresponding season (green coverage in leaf-off and leaf-on season is represented by evergreen coverage and vegetation coverage, respectively), SPC is the standardized $\text{PM}_{2.5}$ concentration of the corresponding season, and SPD is the standardized population density. The $\text{PM}_{2.5}$ concentration was standardized as $SPC = (PC - PC_{min})/(PC_{max} - PC_{min})$ (Morani et al., 2011), where PC is the $\text{PM}_{2.5}$ concentration. PC_{min} and PC_{max} were set as the smaller of the minimum and the larger of the maximum $\text{PM}_{2.5}$ concentration in the GIS map of the leaf-on and leaf-off seasons, respectively, to compare the GD between the two seasons. Population density was standardized as $SPD = (PD - PD_{min})/(PD_{max} - PD_{min})$, where PD is the population density and PD_{min} and PD_{max} are the lowest and highest population densities, respectively.

The annual GDI was weighted by the duration of the two seasons:

$$I_A = (I_{leaf-on} \times t_{leaf-on} + I_{leaf-off} \times t_{leaf-off})/12 \quad (2)$$

where I_A is the annual GDI score and $I_{leaf-on}$ and $I_{leaf-off}$ are the GDI scores of the leaf-on and leaf-off seasons, respectively. $t_{leaf-on}$, $t_{leaf-off}$, and 12 are the number of months in the leaf-on season, leaf-off season, and a year, respectively.

2.2. Case study

The study area is located within the 6th Ring Road of Beijing, China, which covers an area of 2268 km^2 (Fig. 1). Beijing has a typical semi humid continental monsoon climate, with hot and rainy summers, cold and dry winters, and short springs and autumns. The annual precipitation is approximately 600 mm (Zhai et al., 2014), with 80% of the precipitation concentrated in June, July, and August. According to plant phenology, the leaf-on season lasts for 7 months from April to October.

Beijing has experienced rapid urbanization in the last 40 years (Li et al., 2015). Five ring roads were built in 1992, 1999, 2001, 2003, and 2009 (Fig. 1), representing urban expansion in Beijing. Therefore, referring to the five ring roads (2–6), we divide the study area into five subregions (-2, 2–3, 3–4, 4–5, and 5–6) to study the change in GD along the urban-suburban gradient. Because the difficulty of greening varies greatly by land-cover types, it is of great significance to clarify the GD in each of them for predicting the implementation difficulty of a tree planting scheme. Six land-cover types of forest, water, impervious, grassland, farmland, and bare soil were classified (Fig. 2a). The total user accuracy was 91.5%, and the Kappa coefficient was 0.88.

GIS maps of green coverage in the leaf-off and leaf-on seasons are shown in Fig. 2b. A dimidiate pixel model was used to estimate vegetation coverage (Xiao and Moody, 2005). The normalized difference vegetation index (NDVI) data for calculating vegetation coverage were derived from the cloud-free Landsat 8 image on May 18, 2015. Vegetation coverage was calculated as follows:

$$f_c = (NDVI_{May} - NDVI_{min})/(NDVI_{max} - NDVI_{min}) \quad (3)$$

where f_c is the vegetation coverage; $NDVI_{May}$ is the NDVI value in May; $NDVI_{max}$ is the maximum NDVI value in May, representing the NDVI value of pure vegetation pixels; and $NDVI_{min}$ is the minimum NDVI value in May, representing the NDVI value of bare soil.

The NDVI data for calculating evergreen coverage were derived from

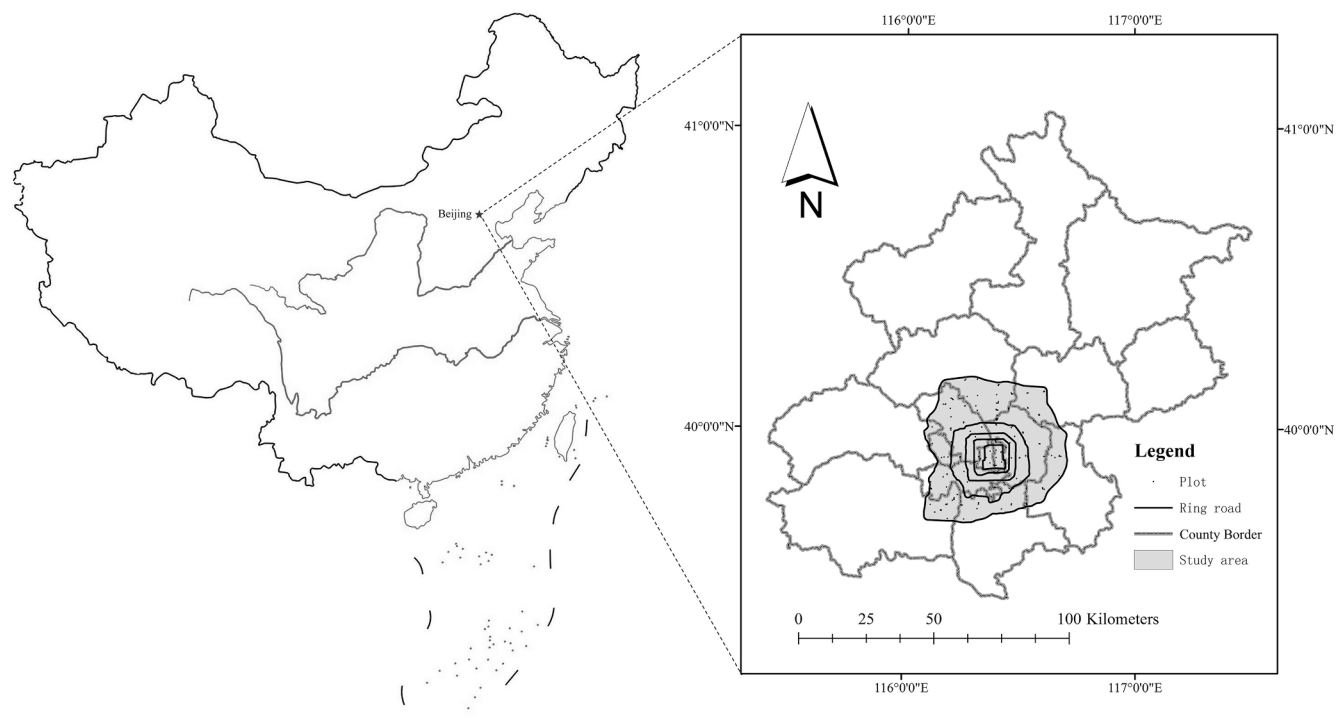


Fig. 1. The study area, plot sites, and the five ring roads of Beijing. The 2_6 ring roads are depicted from the inside out.

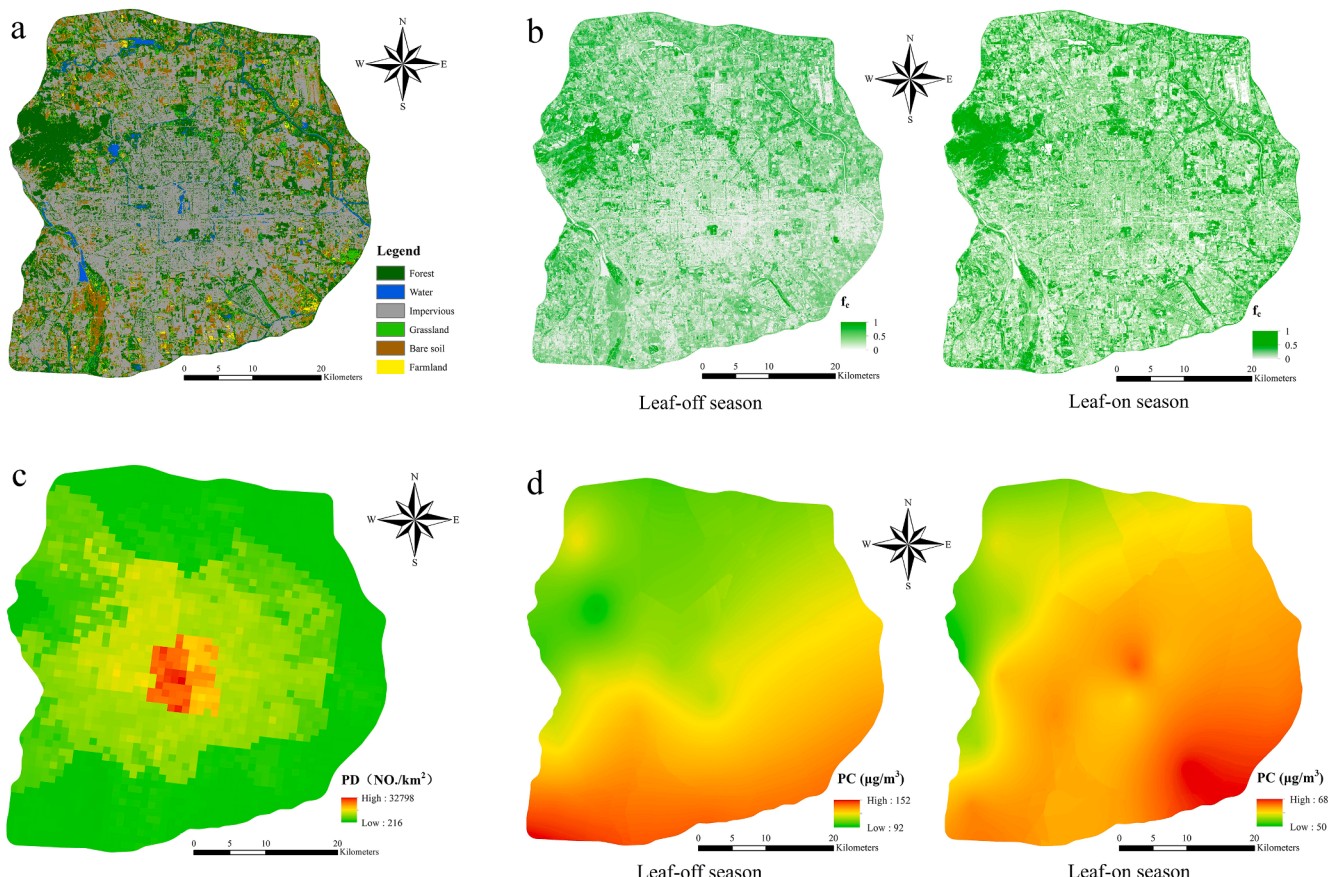


Fig. 2. GIS maps of the (a) land-cover classification, (b) green coverage, (c) population density, and (d) PM_{2.5} concentration of the study area. Green coverage in the leaf-off and leaf-on seasons indicates evergreen coverage and vegetation coverage, respectively.

the cloud-free Landsat 8 image on January 10, 2015. Because only a small difference in NDVI was noted between January and May in evergreen forests (Qiao et al., 2016; Yang et al., 2019), we assumed it to be constant. Thus, the coverage of evergreen species was calculated as:

$$f_{evg} = (NDVI_{Jan} - NDVI_{min}) / (NDVI_{max} - NDVI_{min}) \quad (4)$$

where f_{evg} is the evergreen coverage and $NDVI_{Jan}$ is the NDVI value in January.

Assuming that deciduous and evergreen vegetation covers do not overlap, the coverage of deciduous vegetation was calculated as follows:

$$f_{dec} = f_c - f_{evg} \quad (5)$$

where f_{dec} is the coverage of deciduous vegetation.

A total of 250 (3×3 pixels) plots were randomly selected as accuracy test samples of vegetation coverage. Linear fitting was performed using the visual coverage from Google Earth images in August 2015, the determination coefficient R^2 was 0.64, and the root-mean-square error was 0.20.

The GIS map of the population density is shown in Fig. 2c. The population density distribution data in 2015 were obtained from the Resource and Environment Data Cloud Platform (Xu, 2017). As the cell size of the data was $1 \text{ km} \times 1 \text{ km}$, it was resampled to 30 m in ArcGIS 10.6 (ESRI, CA, USA) to match the vegetation coverage and $\text{PM}_{2.5}$ concentration data. No seasonal variation was assumed in population density.

GIS maps of the $\text{PM}_{2.5}$ concentration in the leaf-off and leaf-on seasons are shown in Fig. 2d. The $\text{PM}_{2.5}$ distribution was obtained by ordinary Kriging interpolation. First, the average concentrations during the leaf-off and leaf-on seasons of 2015 at all 30 environmental air quality monitoring stations were calculated using the data from the China National Environmental Monitoring Center (<http://106.37.208.233:20035/>). Then, Kriging interpolation was performed in ArcGIS 10.6 to obtain the GIS map of $\text{PM}_{2.5}$ pollution during the two seasons. The cell size was set at 30 m to match the resolution of the green coverage data.

2.3. Calculation of contributions to the GDD

GDD includes the difference in the urban-suburban gradient (urban-suburban GDD) and the difference between the leaf-on and leaf-off seasons (seasonal GDD). To better guide urban greening, the green coverage contributions of different land-covers were calculated separately. According to Eq. (1), the contribution value to GDI for each factor was calculated as $Cv = Sv/3$, where Cv is the contribution value and Sv is the standardized value.

Subregion 5–6 was set as the datum for urban-suburban GDD calculation. Then, the contribution to urban-suburban GDD was calculated as follows:

$$UCr_{i \sim 5-6} = (Cv_i - Cv_{(5-6)}) / (I_{Ai} - I_{A(5-6)}) \times 100\% \quad (6)$$

where $UCr_{i \sim 5-6}$ is the contribution rate to the urban-suburban GDD, Cv_i is the contribution value of subregion i, $Cv_{(5-6)}$ is the contribution value of subregion 5–6, I_{Ai} is the annual GDI score of subregion i, and $I_{A(5-6)}$ is the annual GDI score of subregion 5–6.

The leaf-on season was set as the datum for seasonal GDD calculation. Then, the contribution to seasonal GDD was calculated as follows:

$$SCr = (Cv_{leaf-off} - Cv_{leaf-on}) / (I_{leaf-off} - I_{leaf-on}) \times 100\% \quad (7)$$

where SCr is the contribution rate to the seasonal GDD, and $Cv_{leaf-off}$ and $Cv_{leaf-on}$ are the contribution values of the leaf-off and leaf-on seasons, respectively.

2.4. Three tree planting scenarios

A tree-protecting project is being implemented in Beijing, with different woodland coverage goals in different functional areas. The woodland coverage goals of the urban environment protection forest area, the Taihang Mountain scenic forest and industrial development area, and the plain protection forest area are 20.2%, 68.8%, and 24.2%, respectively. The area ratios of the three functional areas are 89.2%, 7.1%, and 3.7%, respectively (BGGB, 2012). To achieve the woodland coverage goal, potential spaces in various types of land may be needed for tree planting. We regarded all spaces without vegetation, except water bodies, as potential candidates (McDonald et al., 2007). To simulate a more reasonable tree planting scheme, we set 20% as the utilization ratio of potential spaces in impervious (Currie and Bass, 2008) and 50% in forest, grassland, farmland, and bare soil. On this basis, to explore the effects of tree composition on $\text{PM}_{2.5}$ reduction and green distribution, three tree planting scenarios were simulated. They are planting all with evergreen trees (Scenario 1), all with deciduous trees (Scenario 2), and with both kinds of current tree compositions (Scenario 3). The composition of tree species in the tree planting scenarios was derived from the plot survey conducted in 2010, and the proportion of evergreen trees was derived from remote sensing data in 2015.

2.5. Estimation of trees' effects on $\text{PM}_{2.5}$

The effects of trees on $\text{PM}_{2.5}$ were calculated using i-Tree Eco v6 (USDA Forestry Service, WA, USA) (i-Tree, 2019). The model calculation was based on the sample survey data collected in 2010 (assuming that the species composition of urban forest has been stable in recent years) and the meteorological and pollution data of 2013 (the only year these data are available for Beijing in the i-Tree Eco database). Then, based on the ratio of total exposure, the $\text{PM}_{2.5}$ removal amount of 2015 was derived from the results of 2013.

In the field survey, a total of 186 woodland plots ($20 \text{ m} \times 20 \text{ m}$) were investigated (Fig. 1), including a total of 2677 trees, of which 624 trees of 10 species were evergreen trees and 2053 trees of 48 species were deciduous trees. The survey items and plot number and size were based on the i-Tree Eco field manual (i-Tree, 2019).

The removal amount of $\text{PM}_{2.5}$ by plants is closely related to precipitation and wind speed (Hirabayashi et al., 2014). Assuming that the climate of the two years was the same, the removal amount depended on the total exposure to $\text{PM}_{2.5}$. Then, the $\text{PM}_{2.5}$ removal amount of 2015 was calculated as $q_{2015} = q_{2013} \times \frac{C_{2015}}{C_{2013}} \times \frac{t_{2015}}{t_{2013}}$, where q_{2015} and q_{2013} are the annual $\text{PM}_{2.5}$ removal amounts in 2015 and 2013, respectively. For evergreen trees, C_{2015} and C_{2013} are the annual average $\text{PM}_{2.5}$ concentrations in the precipitation-free periods of 2015 and 2013, and t_{2015} and t_{2013} are the annual precipitation-free hours of 2015 and 2013, respectively. The removal amount in the two seasons was also allocated based on the total exposure $q_s = q_{2015} \times \frac{C_s}{C_{2015}} \times \frac{t_s}{t_{2015}}$, where q_s is the $\text{PM}_{2.5}$ removal amount of an individual tree in the leaf-on or leaf-off season, C_s and t_s are the average $\text{PM}_{2.5}$ concentration and the precipitation-free hours of the corresponding season, respectively. Only leaves were considered to remove $\text{PM}_{2.5}$ in the i-Tree model (Hirabayashi et al., 2014). Therefore, for deciduous trees, it was assumed that all $\text{PM}_{2.5}$ removal occurred in the leaf-on season. Then, C_{2015} and C_{2013} are the average $\text{PM}_{2.5}$ concentrations in the precipitation-free period of the leaf-on season in 2015 and 2013, and t_{2015} and t_{2013} are the precipitation-free hours of the leaf-on season in 2015 and 2013, respectively. Meteorological and $\text{PM}_{2.5}$ concentration data from 2015 were obtained from the Beijing Capital International Airport weather station (<http://rp5.ru/>) and China National Environmental Monitoring Center (<http://106.37.208.233:20035/>), respectively.

The annual $\text{PM}_{2.5}$ removal amount per unit area by evergreen or deciduous trees was calculated as follows:

$$Q_u = \sum_{i=1}^n \frac{q_i}{CA_i}/n \quad (8)$$

where Q_u is the annual PM_{2.5} removal amount of trees per unit area (t), q_i is the annual PM_{2.5} removal amount of an individual tree in the sample plots (calculated in i-Tree) (t), CA_i is the crown area of the tree (calculated in i-Tree) (m²), and n is the number of trees in the sample plots.

The annual PM_{2.5} removal amount by evergreen or deciduous trees in the study area was calculated separately by multiplying the removal amount per unit area by the total vegetation area:

$$Q = Q_u \times A \times r \times f \quad (9)$$

where Q is the annual PM_{2.5} removal amount of trees in the study area (t), A is the area of the study area (m²), r is the area ratio of forest in the study area, and f is the corresponding coverage of the two tree types in forest areas. The annual PM_{2.5} removal amount by trees was calculated as the sum of PM_{2.5} removed by evergreen and deciduous trees.

The hourly removal rate of atmospheric PM_{2.5} by trees was calculated as follows (Nowak et al., 1998):

$$E = Q_t/(Q_t + Q_s) \quad (10)$$

where E is the average hourly PM_{2.5} removal rate (%), Q_t is the PM_{2.5} removed by trees (t) over a study period, and Q_s is the cumulative hourly atmospheric PM_{2.5} storage (t) over the corresponding time. Q_s was calculated as $Q_s = \sum_{i=1}^n (10^{-3} C_i H_i t_i A)$ (Nowak et al., 2006), where n is the number of months in the study period, C_i is the average PM_{2.5} concentration (μg/m³) in precipitation-free hours in month i, H_i is the average atmospheric boundary layer height (km) in month i (Tang et al., 2016), t_i is the number of precipitation-free hours in month i, and A is the area (km²) of the study area.

The effects of the tree planting scheme on the spatial distribution of PM_{2.5} could not be calculated due to the unclear spatial influence range of trees on PM_{2.5}. Therefore, only the effects on the temporal distribution of PM_{2.5} were calculated. The removal rate of seasonal PM_{2.5} concentration differences referred to the ratio of seasonal PM_{2.5} concentration differences before and after implementing the tree planting scenarios. It was calculated as $R = 1 - \frac{C_{leaf-off} \times (1 - R_{leaf-off}) - C_{leaf-on} \times (1 - R_{leaf-on})}{C_{leaf-off} - C_{leaf-on}} \times 100\%$, where R is the removal rate of the seasonal PM_{2.5} concentration difference, $C_{leaf-on}$ and $C_{leaf-off}$ are the average PM_{2.5} concentrations of the leaf-on and leaf-off seasons, respectively, and $R_{leaf-on}$ and $R_{leaf-off}$ are the PM_{2.5} removal rates of the newly planted trees in the leaf-on and leaf-off seasons, respectively. After simplification, we have the following expression:

$$R = \frac{C_{leaf-off} \times R_{leaf-off} - C_{leaf-on} \times R_{leaf-on}}{C_{leaf-off} - C_{leaf-on}} \times 100\% \quad (11)$$

To alleviate the seasonal difference, R should be larger than 0. $C_{leaf-off}$ is always larger than $C_{leaf-on}$, which means $C_{leaf-off} \times R_{leaf-off} - C_{leaf-on} \times R_{leaf-on} > 0$. $R_{leaf-off}$ and $R_{leaf-on}$ were proportionally contributed by evergreen and deciduous trees. Assuming that the coverage ratio of evergreens in the newly planted trees is r, then the coverage ratio of deciduous trees is $1 - r$. $R_{leaf-off}$ and $R_{leaf-on}$ were calculated as $R_{leaf-off} = R_{leaf-off(S1)} \times r + R_{leaf-off(S2)} \times (1 - r)$ and $R_{leaf-on} = R_{leaf-on(S1)} \times r + R_{leaf-on(S2)} \times (1 - r)$, respectively, where $R_{leaf-off(S1)}$, $R_{leaf-off(S2)}$, $R_{leaf-on(S1)}$, and $R_{leaf-on(S2)}$ are the additional PM_{2.5} removal rates in the leaf-off and leaf-on seasons with tree planting scenarios 1 and 2, respectively. Combining the above three equations, the minimum coverage ratio of evergreen trees to alleviate the seasonal PM_{2.5} concentration difference was obtained as follows:

$$r > \frac{C_{leaf-on} \times R_{leaf-on(S2)} - C_{leaf-off} \times R_{leaf-off(S2)}}{C_{leaf-off} \times (R_{leaf-off(S1)} - R_{leaf-off(S2)}) - C_{leaf-on} \times (R_{leaf-on(S1)} - R_{leaf-on(S2)})} \quad (12)$$

3. Results

3.1. The GD distribution in Beijing

The GDI decreases along the urban-suburban gradient (Fig. 3), with average GDIs of 0.61, 0.53, 0.48, 0.45, and 0.38 in the five subregions, respectively. In different land-cover types, the average GDI values of impervious, bare soil, grassland, farmland, and forest were 0.47, 0.43, 0.35, 0.34, and 0.32, respectively. The GDI value of the entire study area was 0.41, which was smaller than that of all subregions within the 5th ring road and land-cover types of impervious and bare soil. Based on the simulated tree planting scheme, to achieve the woodland coverage goal of 2020, potential spaces with GDIs larger than 0.48 should be utilized. Priority greening areas are illustrated in Fig. 3.

3.2. Contributions to the GDD

Population density contributed the most to the urban-suburban GDD, accounting for approximately three-fourths on average, and the contribution decreased in the urban-suburban gradient (Table 1). The PM_{2.5} concentration had no distinct effect on the urban-suburban GDD. The second contributor was the green coverage of the impervious land-cover type, accounting for more than half. Green coverage in forest, grassland, farmland, and bare soil had negative contributions to the urban-suburban GDD.

The primary factor driving the seasonal GDD was the PM_{2.5} concentration, accounting for more than two-thirds of variability for the entire study area (Table 2). Under the assumption of no seasonal variation, population density did not contribute to the seasonal difference. Among the contributions from green coverage of different land-cover types, forest contributed the most, followed by impervious, and the remaining types all contributed less than 5%.

3.3. Effects of trees on PM_{2.5}

In 2015, the PM_{2.5} removed by trees in the study area was 453.6 t, of which 283.0 t was in the leaf-on season and 170.6 t was in the leaf-off season (Fig. 4a). By type, 287.4 t was removed by evergreen trees and 166.2 t by deciduous trees. The air quality improvement rates annually, during the leaf-on season, and during the leaf-off season were 0.047%, 0.062%, and 0.034%, respectively (Fig. 4b). The PM_{2.5} removal efficiency of evergreen trees was approximately 2.7 times that of deciduous trees, i.e., 14.6 kg/ha/yr and 5.5 kg/ha/yr, respectively.

Planting all with evergreen trees was the most effective scenario for removing atmospheric PM_{2.5} (Fig. 4). An additional 121.7 t PM_{2.5} could be removed annually in Scenario 1, compared with 45.7 t and 74.5 t in Scenarios 2 and 3, with additional removal rates of 0.012%, 0.004% and 0.007%, respectively. The difference was not obvious in the leaf-on season; an additional 49.5 t, 45.7 t, and 46.5 t PM_{2.5} could be removed in Scenarios 1, 2, and 3, respectively, with additional removal rates of 0.011%, 0.010%, and 0.010%, respectively. In the leaf-off season, the difference was obvious; an additional 72.2 t PM_{2.5} could be removed in Scenario 1, compared with 0 t and 28.0 t in Scenarios 2 and 3, with additional removal rates of 0.015%, 0.000%, and 0.006%, respectively.

The maximum effects in alleviating the seasonal difference in PM_{2.5} concentration could reach 0.019% under Scenario 1. In Scenario 2, the seasonal difference in PM_{2.5} concentration would increase by 0.011%. To alleviate the seasonal difference in PM_{2.5} concentration, the coverage ratio of evergreens should be at least 37.1% in the new trees to plant.

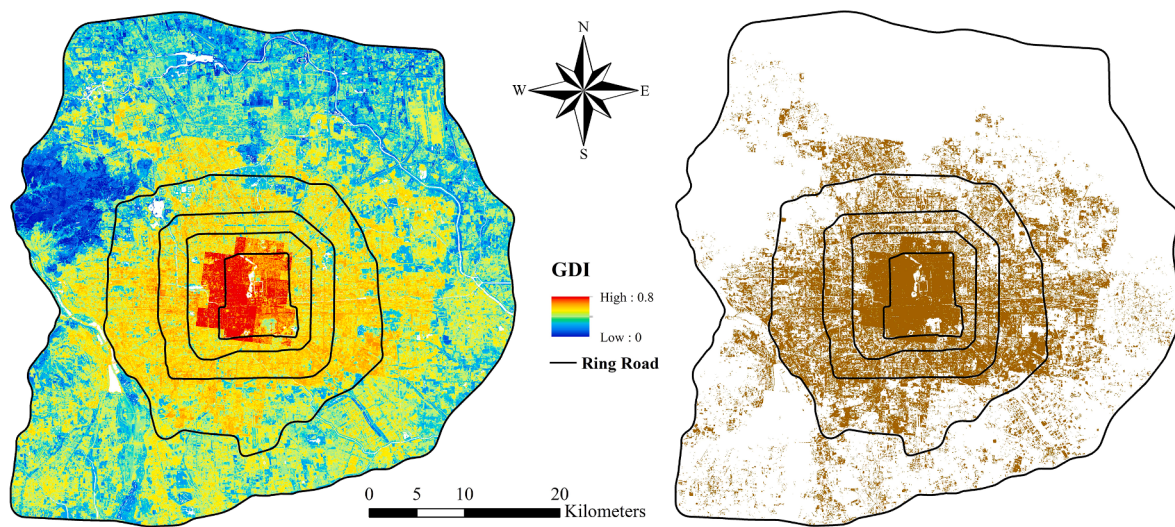


Fig. 3. Maps of GDI and the priority greening area within the 6th ring road in Beijing. Areas with GDI larger than 0.48 are priority areas according to the woodland coverage goal of 2020, as shown on the right side of the figure.

Table 1
Contributions to urban-suburban GDD.

Factor	Contribution rate				
	-2 ~ 5-6	2-3 ~ 5-6	3-4 ~ 5-6	4-5 ~ 5-6	
f_c	Impervious	50.3%	55.3%	73.4%	64.1%
	Forest	-8.1%	-4.8%	-10.2%	-10.9%
	Grassland	-7.2%	-7.9%	-8.1%	-6.0%
	Farmland	-1.9%	-2.2%	-2.7%	-2.9%
$PM_{2.5}$ concentration	Bare soil	-20.1%	-22.4%	-27.6%	-23.9%
		-1.5%	-1.1%	2.6%	7.6%
Population density		88.5%	83.1%	72.6%	72.0%
Total		100%	100%	100%	100%

f_c represents green coverage.

3.4. Impact of tree planting on green distribution

The green coverage clearly changed after implementing tree planting plan (Fig. 5). Total vegetation coverage now increases along the urban-suburban gradient (Fig. 5a). With our tree planting scenarios in the selected priority area, the total vegetation coverage was distributed almost uniformly between subregions (Fig. 5b, c, d). In Scenario 1, the evergreen vegetation coverage in the city center increased more than in the peripheral areas, resulting in a weak downward trend in the urban-suburban gradient (Fig. 5b). In Scenario 2, the deciduous vegetation coverage in the city center was much higher than that in the periphery, which aggravated the uneven distribution of deciduous vegetation

(Fig. 5c). In Scenario 3, the uneven distribution of evergreen vegetation was alleviated, but the uneven distribution of deciduous vegetation was aggravated (Fig. 5d).

The seasonal GS coverage difference can be seen as deciduous vegetation coverage. In the current situation, little difference in deciduous coverage exists between subregions (Fig. 5a). In Scenario 1, the seasonal differences remained unchanged (Fig. 5b). In Scenario 2, the seasonal differences in all subregions increased, and the rate of increase decreased along the urban-suburban gradient (Fig. 5c). In Scenario 3, the seasonal differences increased to a lesser extent, with a similar increasing trend as Scenario 2 (Fig. 5d).

4. Discussion

By 2050, 70% of the world's population of approximately 6.68 billion people is estimated to live in cities (UN, 2018). A good urban environment is crucial for human development. Increasing GS is fundamental for improving urban environmental quality (Bolund and Hunhammar, 1999). Considering the scarcity of vacant lands in urban areas and the long-term process of greening, to achieve higher land-use efficiency, finding priority spaces is a challenge. A method based on the relationship between ES supply and demand will achieve higher ES benefits. ES supply and demand are negatively correlated not only in space (Wang et al., 2019b; Xu et al., 2020) but also in time at the seasonal scale. However, previous studies to find space for greening mostly ignored the spatiotemporal changes in ES supply and demand, especially between seasons. Without considering the seasonal variation, the GD will be underestimated in areas with deciduous vegetation coverage. Based on the relationship between supply and demand for $PM_{2.5}$

Table 2
Contributions to seasonal GDD.

Factor	Contribution rate					
	-2	2-3	3-4	4-5	5-6	Holistic
f_c	Impervious	17.5%	16.0%	13.9%	9.7%	6.0%
	Forest	13.1%	15.2%	13.2%	14.5%	18.5%
	Grassland	0.2%	0.5%	0.9%	1.8%	2.7%
	Farmland	0.0%	0.0%	0.1%	0.2%	0.7%
	Bare soil	0.1%	0.2%	0.2%	0.6%	1.3%
$PM_{2.5}$ concentration		69.1%	68.1%	71.7%	73.2%	70.8%
Population density		0.0%	0.0%	0.0%	0.0%	0.0%
Total		100%	100%	100%	100%	100%

f_c represents green coverage.

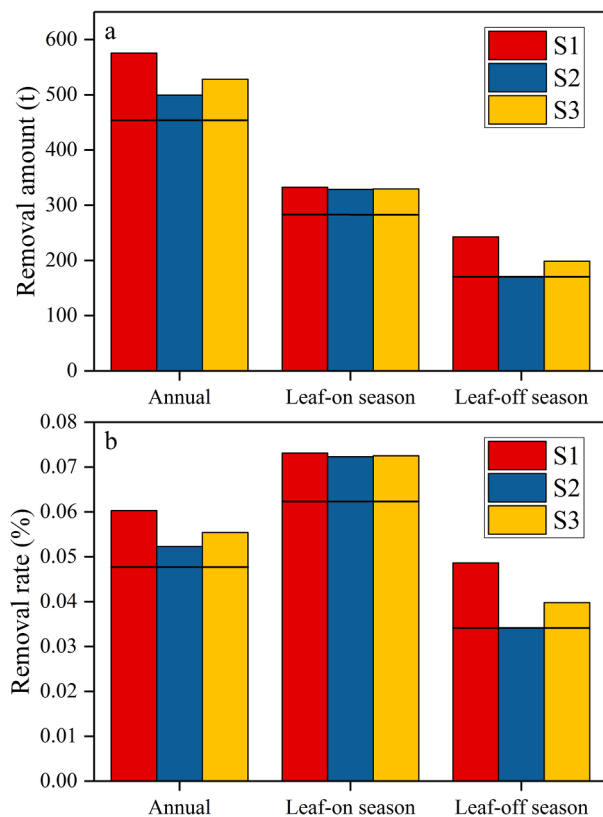


Fig. 4. Effects of trees on atmospheric PM_{2.5} removal in different time periods. Subgraphs a and b show the PM_{2.5} removal amount and removal rate by trees, respectively. S1, S2, and S3 represent three tree planting scenarios (all with evergreen trees, all with deciduous trees, and with the current tree composition, respectively). The horizontal solid lines indicate the effect of trees before tree planting.

removal, GDI was proposed to find priority spaces for greening.

In Beijing, the GD is larger in the city center than in the peripheral areas, with a greening distribution pattern similar to that in other studies in Baltimore (Bodnaruk et al., 2017; Locke et al., 2013). In addition, this pattern is also similar to the demand for energy, food, and water in Leipzig–Halle (Kroll et al., 2012) and the integrated ES demand in Trento (Cortinovis and Geneletti, 2020). Within a city, the ES value gradually increases from the center to the edge (Xu et al., 2020), which is closely related to the development model of cities. The traditional urban development model is described as “making a pancake”. All of the expanding construction is centered around the old city areas. A large population agglomerates in the city center, and the original GS is gradually encroached by artificial infrastructures (Brunner and Cozens,

2013; Nowak and Greenfield, 2020). With the further expansion of cities, an increasing number of environmental problems have appeared (Shi et al., 2020), accompanied by the growing demand for GS (Haaland and van den Bosch, 2015). This in turn, forces us to increase GS in cities.

While paying attention to the demand for ESs, we also want to clarify the causes of GDD in time and space, which are closely related to environmental equity. Although equal weight is given to the three factors when calculating GDI, they do not contribute equally to the urban-suburban and seasonal GDD. The spatial difference is mostly related to the rapid decrease in population density in the urban-suburban gradient, and the seasonal difference is mostly related to the large difference in PM_{2.5} concentration in the leaf-off and leaf-on seasons. GS has limited effects on PM_{2.5} concentrations (Nowak et al., 2013), and competes with human beings for space (Brunner and Cozens, 2013). To reduce the GD and relieve the difference both in time and space, only greening is inadequate, pollution control and population relieving measures should be put into practice simultaneously. According to the Beijing Master Plan 2016–2035 (PGBM, 2017), Beijing is organizing a special campaign named “relief and renovation and promotion” throughout the city. One of its goals is to reduce the population density in central urban areas. The target for PM_{2.5} concentration has also been quantified in the Master Plan. This campaign will be very helpful in lowering the GDD. In the contribution of green coverage to GDD, impervious areas contribute considerably to urban-suburban and seasonal GDD, which verifies the importance of greening in these areas. In addition, although the forest has a lower priority for greening, it contributes more to the seasonal GDD than other land-cover types. Considering the spillover effect of ESs (Bolund and Hunhammar, 1999; Lin et al., 2020), attention should also be paid to evergreen greening in urban forests, which is often overlooked.

Provision space for greening in compact cities is a significant challenge (Haaland and van den Bosch, 2015). Currently, most of the new GS in Beijing is transferred from farmlands (Yao et al., 2019). The remaining farmland area in the study area is very small, and almost all of them are distributed in the periphery. With the current land-use conversion strategy, the potential space for green is far from sufficient. Among the six land-cover types, impervious land has the highest GDI and contributes considerably to the GDD; it is the key area for greening. However, in the calculation of GDI, spaces without vegetation are all considered potential candidates, focusing more on the importance of potential spaces rather than availability. Reducing the impervious areas is the biggest obstacle to providing GS (Wang et al., 2020). In the urban areas, roofs usually comprise 40–50% of the impervious area (Dunnett and Kingsbury, 2008), which provides ample potential space for greening. Green roofs may be an appropriate choice for impervious greening. However, focus should be placed on the difference between green roofs and woodlands in providing ESs.

In addition to finding space for greening, the selection of greening species has also received much attention. It is well known that evergreen

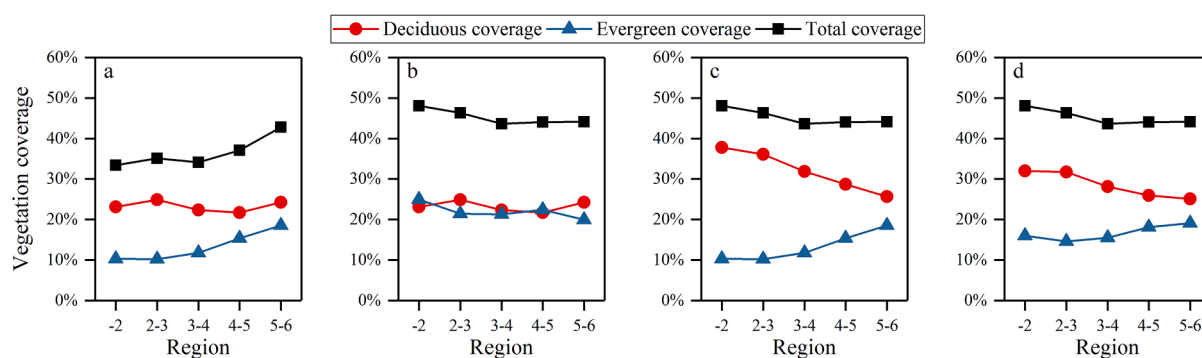


Fig. 5. Vegetation coverage changes in the urban-suburban gradient under different tree planting scenarios. Subgraph a shows the current status, and subgraphs b, c, and d show tree planting scenarios 1, 2, and 3, respectively.

trees are more efficient than deciduous trees for removing atmospheric PM_{2.5} (Fusaro et al., 2017; García de Jalón et al., 2019). The results of our study also confirm this. In addition, considering the seasonal difference in ES supply in greening will inevitably highlight the role of evergreen trees. As shown in the results, they are indispensable in alleviating the seasonal PM_{2.5} difference. A safe and stable environment is of great significance to the production and life of urban residents. Moreover, planting evergreen vegetation in the priority areas selected in this study can effectively alleviate the uneven distribution of green vegetation both in time and space. Green is the foundation of ESs (Bolund and Hunhammar, 1999), and a relatively uniform distribution of green will help to alleviate environmental inequity. All in all, evergreen trees are recommended for greening in Beijing.

Several aspects of our study need to be improved. First, PM_{2.5} removed by shrubs and herbs is not covered in this work. Although they cannot be compared with trees in removing PM_{2.5}, they still play an important role (Chen et al., 2019a; Gopalakrishnan et al., 2018). Second, supplementing the i-Tree database of the studied area will greatly simplify and accurately calculate the effect of trees on PM_{2.5}. Third, higher-resolution remote sensing images should be used in city studies (Welch, 1982), as some small woodlands cannot be recognized at the current resolution, which may lead to an underestimation of woodland coverage.

Tree planting as well as the seasonal variation not only change the coverage of GS but also the landscape pattern, which has important impacts on PM_{2.5} (Chen et al., 2019b; Lei et al., 2018; Shi et al., 2019). In addition, even though the deposition effect dominates over the dispersion effect at the urban scale (Jeanjean et al., 2016; Tiwari and Kumar, 2020), at a smaller scale, trees may hinder the diffusion of pollutants, resulting in increased concentration (Jin et al., 2014; Morakinyo and Lam, 2016). More specific selection of tree planting locations at a small scale should simulate the aerodynamic dispersion effect. Urban greening is a very complex project and only considering the removal of PM_{2.5} is inadequate for identifying the priority greening space. Other ESs and Disservices should also be considered (Bodnaruk et al., 2017). Only with multiple objectives can more benefits be realized from urban greening (Vallecillo et al., 2018). In addition, trees go through the processes of growth, maturity, and death, accompanied by a change in ES delivery (Morani et al., 2011; Parsa et al., 2019). Taking these processes into account will be meaningful for the long-term planning of urban GS.

5. Conclusions

Based on the spatiotemporal variation in the relationship between the supply and demand of PM_{2.5} removal, a GDI was proposed to find the priority spaces for greening by combining seasonal nongreen coverage, PM_{2.5} concentration, and population density. Without considering the seasonal variation in ES supply and demand, the GD will definitely be underestimated in areas with deciduous vegetation coverage. In Beijing, GD increases in the suburban-urban gradient and is higher in the impervious areas than in other land-cover types. Greening in the impervious areas is the key to alleviating the urban-suburban GDD, and evergreen greening in the forest and impervious areas is crucial to alleviate the seasonal GDD. In addition to the obvious GD in impervious areas, attention should also be paid to the often overlooked evergreen greening in urban forests. Evergreen trees are more efficient in removing PM_{2.5} than deciduous trees, and they are also indispensable in alleviating the seasonal PM_{2.5} concentration difference and the uneven distribution of GS. Thus, evergreen trees are recommended for greening in Beijing.

CRediT authorship contribution statement

Rui Zhang: Conceptualization, Writing - original draft, Writing - review & editing. **Guojian Chen:** Software, Data curation. **Zhe Yin:** Investigation, Methodology. **Yuxin Zhang:** Methodology, Writing -

review & editing. **Keming Ma:** Conceptualization, Writing - review & editing.

Declaration of Competing Interest

The authors declare that they have no known competing financial interests or personal relationships that could have appeared to influence the work reported in this paper.

Acknowledgment

This work was supported by the Key Project of the National Natural Science Foundation of China (41430638).

References

- Bealey, W.J., McDonald, A.G., Nernitz, E., Donovan, R., Dragosits, U., Duffy, T.R., Fowler, D., 2007. Estimating the reduction of urban PM10 concentrations by trees within an environmental information system for planners. *J. Environ. Manage.* 85, 44–58. <https://doi.org/10.1016/j.jenvman.2006.07.007>.
- BGGB (Beijing Gardening and Greening Bureau), 2012. Beijing Woodland Protection and Utilization Plan (2010–2020). Retrieved September 15, 2018 from <http://ylhbj.beijing.gov.cn/>.
- Bodnaruk, E.W., Kroll, C.N., Yang, Y., Hirabayashi, S., Nowak, D.J., Endreny, T.A., 2017. Where to plant urban trees? A spatially explicit methodology to explore ecosystem service tradeoffs. *Landscape. Urban Plan.* 157, 457–467. <https://doi.org/10.1016/j.landurbplan.2016.08.016>.
- Bolund, P., Hunhammar, S., 1999. Ecosystem services in urban areas. *Ecol. Econ.* 29, 293–301. [https://doi.org/10.1016/S0921-8009\(99\)00013-0](https://doi.org/10.1016/S0921-8009(99)00013-0).
- Brunner, J., Cozens, P., 2013. 'Where Have All the Trees Gone?' Urban consolidation and the demise of urban vegetation: a case study from Western Australia. *Plan. Pract. Res.* 28, 231–255. <https://doi.org/10.1080/02697459.2012.733525>.
- Chen, M., Dai, F., Yang, B., Zhu, S., 2019a. Effects of neighborhood green space on PM2.5 mitigation: evidence from five megacities in China. *Build. Environ.* 156, 33–45. <https://doi.org/10.1016/j.buildenv.2019.03.007>.
- Chen, M., Dai, F., Yang, B., Zhu, S., 2019b. Effects of urban green space morphological pattern on variation of PM2.5 concentration in the neighborhoods of five Chinese megacities. *Build. Environ.* 158, 1–15. <https://doi.org/10.1016/j.buildenv.2019.04.058>.
- Chen, W., Yan, L., Zhao, H., 2015. Seasonal variations of atmospheric pollution and air quality in Beijing. *Atmosphere* 6, 1753–1770. <https://doi.org/10.3390/atmos6111753>.
- Cortinovis, C., Geneletti, D., 2020. A performance-based planning approach integrating supply and demand of urban ecosystem services. *Landscape. Urban Plan.* 201, 103842. <https://doi.org/10.1016/j.landurbplan.2020.103842>.
- Currie, B.A., Bass, B., 2008. Estimates of air pollution mitigation with green plants and green roofs using the UFORE model. *Urban Ecosyst.* 11, 409–422. <https://doi.org/10.1007/s11252-008-0054-y>.
- Dunnett, N., Kingsbury, N., 2008. *Planting Green Roofs and Living Walls*. Timber press Portland, OR.
- Fusaro, L., Marando, F., Sebastiani, A., Capotorti, G., Blasi, C., Copiz, R., Congedo, L., Munaro, M., Ciancarella, L., Manes, F., 2017. Mapping and assessment of PM10 and O₃ removal by woody vegetation at urban and regional level. *Remote Sens.* 9, 791. <https://doi.org/10.3390/rs9080791>.
- García de Jalón, S., Burgess, P.J., Curiel Yuste, J., Moreno, G., Graves, A., Palma, J.H.N., Crous-Duran, J., Kay, S., Chibai, A., 2019. Dry deposition of air pollutants on trees at regional scale: A case study in the Basque Country. *Agric. For. Meteorol.* 278, 107648 <https://doi.org/10.1016/j.agrformet.2019.107648>.
- Givoni, B., 1991. Impact of planted areas on urban environmental quality: a review. *Atmos. Environ. Part B. Urban Atmosphere.* 25, 289–299. [https://doi.org/10.1016/0957-1272\(91\)90001-U](https://doi.org/10.1016/0957-1272(91)90001-U).
- Gopalakrishnan, V., Hirabayashi, S., Ziv, G., Bakshi, B.R., 2018. Air quality and human health impacts of grasslands and shrublands in the United States. *Atmos. Environ.* 182, 193–199. <https://doi.org/10.1016/j.atmosenv.2018.03.039>.
- Haaland, C., van den Bosch, C.K., 2015. Challenges and strategies for urban green-space planning in cities undergoing densification: a review. *Urban For. Urban Green.* 14, 760–771. <https://doi.org/10.1016/j.ufug.2015.07.009>.
- Hirabayashi, S., Kroll, C.N., Nowak, D.J., 2014. i-Tree eco dry deposition model descriptions. *Citeseer.*
- i-Tree, 2019. i-Tree: tools for assessing and managing community forests.
- Jeanjean, A.P.R., Monks, P.S., Leigh, R.J., 2016. Modelling the effectiveness of urban trees and grass on PM2.5 reduction via dispersion and deposition at a city scale. *Atmos. Environ.* 147, 1–10. <https://doi.org/10.1016/j.atmosenv.2016.09.033>.
- Jiang, M., Tian, S., Zheng, Z., Zhan, Q., He, Y., 2017. Human activity influences on vegetation cover changes in Beijing, China, from 2000 to 2015. *Remote Sens.* 9, 271. <https://doi.org/10.3390/rs9030271>.
- Jin, S., Guo, J., Wheeler, S., Kan, L., Che, S., 2014. Evaluation of impacts of trees on PM2.5 dispersion in urban streets. *Atmos. Environ.* 99, 277–287. <https://doi.org/10.1016/j.atmosenv.2014.10.002>.

- Kroll, F., Müller, F., Haase, D., Fohrer, N., 2012. Rural–urban gradient analysis of ecosystem services supply and demand dynamics. *Land Use Pol.* 29, 521–535. <https://doi.org/10.1016/j.landusepol.2011.07.008>.
- Lei, Y., Duan, Y., He, D., Zhang, X., Chen, L., Li, Y., Gao, Y., Tian, G., Zheng, J., 2018. Effects of urban greenspace patterns on particulate matter pollution in metropolitan Zhengzhou in Henan, China. *Atmosphere* 9, 199. <https://doi.org/10.3390/atmos9050199>.
- Li, X., Gong, P., Liang, L., 2015. A 30-year (1984–2013) record of annual urban dynamics of Beijing City derived from Landsat data. *Remote Sens. Environ.* 166, 78–90. <https://doi.org/10.1016/j.rse.2015.06.007>.
- Lin, Y., Yang, X., Li, Y., Yao, S., 2020. The effect of forest on PM2.5 concentrations: a spatial panel approach. *Forest Policy. Econ.* 118, 102261 <https://doi.org/10.1016/j.forepol.2020.102261>.
- Locke, D.H., Grove, J.M., Galvin, M., O’Neil-Dunne, J.P., Murphy, C., 2013. Applications of urban tree canopy assessment and prioritization tools: Supporting collaborative decision making to achieve urban sustainability goals. *Cities. Environ.* 6 (1): article 7 6, 1–26. <https://digitalcommons.lmu.edu/cate/vol6/iss1/7>.
- McDonald, A.G., Bealey, W.J., Fowler, D., Dragosits, U., Skiba, U., Smith, R.I., Donovan, R.G., Brett, H.E., Hewitt, C.N., Nemitz, E., 2007. Quantifying the effect of urban tree planting on concentrations and depositions of PM10 in two UK conurbations. *Atmos. Environ.* 41, 8455–8467. <https://doi.org/10.1016/j.atmosenv.2007.07.025>.
- Morakinyo, T.E., Lam, Y.F., 2016. Study of traffic-related pollutant removal from street canyon with trees: dispersion and deposition perspective. *Environ Sci. Pollut Res.* 23, 21652–21668. <https://doi.org/10.1007/s11356-016-7322-9>.
- Morani, A., Nowak, D.J., Hirabayashi, S., Calfapietra, C., 2011. How to select the best tree planting locations to enhance air pollution removal in the MillionTreesNYC initiative. *Environ Pollut.* 159, 1040–1047. <https://doi.org/10.1016/j.envpol.2010.11.022>.
- Navarrete-Hernandez, P., Laffan, K., 2019. A greener urban environment: designing green infrastructure interventions to promote citizens’ subjective wellbeing. *Landscape Urban Plan.* 191, 103618 <https://doi.org/10.1016/j.landurbplan.2019.103618>.
- Nesbitt, L., Meitner, M.J., Girling, C., Sheppard, S.R.J., Lu, Y., 2019. Who has access to urban vegetation? A spatial analysis of distributional green equity in 10 US cities. *Landscape Urban Plan.* 181, 51–79. <https://doi.org/10.1016/j.landurbplan.2018.08.007>.
- Nowak, D.J., Crane, D.E., Stevens, J.C., 2006. Air pollution removal by urban trees and shrubs in the United States. *Urban For. Urban Green.* 4, 115–123. <https://doi.org/10.1016/j.ufug.2006.01.007>.
- Nowak, D.J., Greenfield, E.J., 2020. The increase of impervious cover and decrease of tree cover within urban areas globally (2012–2017). *Urban For. Urban Green.* 49, 126638 <https://doi.org/10.1016/j.ufug.2020.126638>.
- Nowak, D.J., Hirabayashi, S., Bodine, A., Hoehn, R., 2013. Modeled PM2.5 removal by trees in ten U.S. cities and associated health effects. *Environ Pollut.* 178, 395–402. <https://doi.org/10.1016/j.envpol.2013.03.050>.
- Nowak, D.J., McHale, P.J., Ibarra, M., Crane, D., Stevens, J.C., Luley, C.J., 1998. Modeling the effects of urban vegetation on air pollution. Air pollution modeling and its application XII. Springer, pp. 399–407.
- Parsa, V.A., Salehi, E., Yavari, A.R., van Bodegom, P.M., 2019. Analyzing temporal changes in urban forest structure and the effect on air quality improvement. *Sust. Cities Soc.* 48, 151048 <https://doi.org/10.1016/j.scs.2019.101548>.
- PGBM (People’s Government of Beijing Municipality), 2017. Beijing Master Plan 2016–2035. Retrieved April 12, 2018 from <http://www.beijing.gov.cn/>.
- Pham, T.-T.-H., Apparicio, P., Séguin, A.-M., Landry, S., Gagnon, M., 2012. Spatial distribution of vegetation in Montreal: an uneven distribution or environmental inequity? *Landscape Urban Plan.* 107, 214–224. <https://doi.org/10.1016/j.landurbplan.2012.06.002>.
- Qiao, Z., Xu, X., Zhao, M., Wang, F., Liu, L., 2016. The application of a binary division procedure to the classification of forest subcategories using MODIS time-series data during 2000–2010 in China. *Int. J. Remote Sens.* 37, 2433–2450. <https://doi.org/10.1080/01431161.2016.1176269>.
- Shi, G., Lu, X., Deng, Y., Urpelainen, J., Liu, L.C., Zhang, Z., Wei, W., Wang, H., 2020. Air Pollutant Emissions Induced by Population Migration in China. *Environ Sci. Technol.* 54, 6308–6318. <https://doi.org/10.1021/acs.est.0c00726>.
- Shi, Y., Ren, C., Lau, K.K.-L., Ng, E., 2019. Investigating the influence of urban land use and landscape pattern on PM2.5 spatial variation using mobile monitoring and WUDAPT. *Landscape Urban Plan.* 189, 15–26. <https://doi.org/10.1016/j.landurbplan.2019.04.004>.
- Song, C., He, J., Wu, L., Jin, T., Chen, X., Li, R., Ren, P., Zhang, L., Mao, H., 2017. Health burden attributable to ambient PM2.5 in China. *Environ Pollut.* 223, 575–586. <https://doi.org/10.1016/j.envpol.2017.01.060>.
- Tang, G., Zhang, J., Zhu, X., Song, T., Münnkel, C., Hu, B., Schäfer, K., Liu, Z., Zhang, J., Wang, L., Xin, J., Suppan, P., Wang, Y., 2016. Mixing layer height and its implications for air pollution over Beijing, China. *Atmos. Chem. Phys.* 16, 2459–2475. <https://doi.org/10.5194/acp-16-2459-2016>.
- Tian, G., Liu, X., Kong, L., 2018. Spatiotemporal Patterns and Cause Analysis of PM2.5 Concentrations in Beijing, China. *Adv. Meteorol.* 2018, 1724872. 10.1155/2018/1724872.
- Tiwari, A., Kumar, P., 2020. Integrated dispersion-deposition modelling for air pollutant reduction via green infrastructure at an urban scale. *Sci. Total Environ.* 723, 138078 <https://doi.org/10.1016/j.scitotenv.2020.138078>.
- Tiwari, A., Sinnett, D., Peachey, C., Chalabi, Z., Vardoulakis, S., Fletcher, T., Leonard, G., Grundy, C., Azapagic, A., Hutchings, T.R., 2009. An integrated tool to assess the role of new planting in PM10 capture and the human health benefits: a case study in London. *Environ Pollut.* 157, 2645–2653. <https://doi.org/10.1016/j.envpol.2009.05.005>.
- UN, 2018. World urbanization prospects: The 2018 revision. New York.
- Vallecillo, S., Polce, C., Barbosa, A., Perpiña Castillo, C., Vandecasteele, I., Rusch, G.M., Maes, J., 2018. Spatial alternatives for Green Infrastructure planning across the EU: an ecosystem service perspective. *Landscape Urban Plan.* 174, 41–54. <https://doi.org/10.1016/j.landurbplan.2018.03.001>.
- Varol, T., Gormus, S., Cengiz, S., Ozel, H.B., Cetin, M., 2019. Determining potential planting areas in urban regions. *Environ. Monit. Assess.* 191, 157. <https://doi.org/10.1007/s10661-019-7299-1>.
- Wang, A., Wang, H., Chan, E., 2020. The incompatibility in urban green space provision: An agent-based comparative study. *J. Clean Prod.* 253 <https://doi.org/10.1016/j.jclepro.2020.120007>.
- Wang, J., Xu, C., Pauleit, S., Kindler, A., Banzhaf, E., 2019a. Spatial patterns of urban green infrastructure for equity: a novel exploration. *J. Clean Prod.* 238, 117858 <https://doi.org/10.1016/j.jclepro.2019.117858>.
- Wang, J., Zhai, T., Lin, Y., Kong, X., He, T., 2019b. Spatial imbalance and changes in supply and demand of ecosystem services in China. *Sci. Total Environ.* 657, 781–791. <https://doi.org/10.1016/j.scitotenv.2018.12.080>.
- Wang, Y., Ying, Q., Hu, J., Zhang, H., 2014. Spatial and temporal variations of six criteria air pollutants in 31 provincial capital cities in China during 2013–2014. *Environ. Int.* 73, 413–422. <https://doi.org/10.1016/j.envint.2014.08.016>.
- Welch, R., 1982. Spatial resolution requirements for urban studies. *Int. J. Remote Sens.* 3, 139–146. <https://doi.org/10.1080/01431168208948387>.
- Wolch, J.R., Byrne, J., Newell, J.P., 2014. Urban green space, public health, and environmental justice: the challenge of making cities ‘just green enough’. *Landscape Urban Plan.* 125, 234–244. <https://doi.org/10.1016/j.landurbplan.2014.01.017>.
- Wu, C., Xiao, Q., McPherson, E.G., 2008. A method for locating potential tree-planting sites in urban areas: a case study of Los Angeles, USA. *Urban For. Urban Green.* 7, 65–76. <https://doi.org/10.1016/j.ufug.2008.01.002>.
- Xiao, J., Moody, A., 2005. A comparison of methods for estimating fractional green vegetation cover within a desert-to-upland transition zone in central New Mexico, USA. *Remote Sens. Environ.* 98, 237–250. <https://doi.org/10.1016/j.rse.2005.07.011>.
- Xu, Q., Yang, R., Zhuang, D., Lu, Z., 2020. Spatial gradient differences of ecosystem services supply and demand in the Pearl River Delta region. *J. Clean Prod.* 279 <https://doi.org/10.1016/j.jclepro.2020.123849>.
- Xu, X., 2017. Chinese population spatial distribution kilometer grid data set. Data Registration and Publishing System of Data Center of Resources and Environmental Science, Chinese Academy of Sciences, Retrieved June 23, 2018 from <http://www.resdc.cn/>. 10.12078/2017121101.
- Yang, Y., Wu, T., Wang, S., Li, J., Muhammud, F., 2019. The NDVI-CV method for mapping evergreen trees in complex urban areas using reconstructed Landsat 8 time-series data. *Forests* 10, 139. <https://doi.org/10.3390/f10020139>.
- Yao, J., Liu, M., Chen, N., Wang, X., He, X., Hu, Y., Wang, X., Chen, W., 2020. Quantitative assessment of demand and supply of urban ecosystem services in different seasons: a case study on air purification in a temperate city. *Landscape Ecol.* 10.1007/s10980-020-01112-7.
- Yao, N., Konijnendijk van den Bosch, C.C., Yang, J., Devisscher, T., Wirtz, Z., Jia, L., Duan, J., Ma, L., 2019. Beijing’s 50 million new urban trees: strategic governance for large-scale urban afforestation. *Urban For. Urban Green.* 44, 126392 <https://doi.org/10.1016/j.ufug.2019.126392>.
- Zhai, T., Wang, J., Jin, Z., Qi, Y., Fang, Y., Liu, J., 2020. Did improvements of ecosystem services supply-demand imbalance change environmental spatial injustices? *Ecol. Indic.* 111, 106068 <https://doi.org/10.1016/j.ecolind.2020.106068>.
- Zhai, Y., Guo, Y., Zhou, J., Guo, N., Wang, J., Teng, Y., 2014. The spatio-temporal variability of annual precipitation and its local impact factors during 1724–2010 in Beijing, China. *Hydrol. Process.* 28, 2192–2201. <https://doi.org/10.1002/hyp.9772>.
- Zhao, X., Zhou, W., Han, L., Locke, D., 2019. Spatiotemporal variation in PM2.5 concentrations and their relationship with socioeconomic factors in China’s major cities. *Environ. Int.* 133, 105145 <https://doi.org/10.1016/j.envint.2019.105145>.
- Zhong, J., Li, Z., Sun, Z., Tian, Y., Yang, F., 2020. The spatial equilibrium analysis of urban green space and human activity in Chengdu, China. *J. Clean Prod.* 259, 120754 <https://doi.org/10.1016/j.jclepro.2020.120754>.
- Zhu, G., Hu, W., Liu, Y., Cao, J., Ma, Z., Deng, Y., Sabel, C.E., Wang, H., 2019. Health burdens of ambient PM2.5 pollution across Chinese cities during 2006–2015. *J. Environ. Manage.* 243, 250–256. <https://doi.org/10.1016/j.jenvman.2019.04.119>.